Surface Classification from Aircraft Icing Droplet Splash Images

Xueqing Zhang, Stuart Barnes and David W. Hammond

***Abstract*— The build up of water ice on aircraft flight surfaces poses a significant safety risk. As a result, much effort has gone into studying this problem in order to understand how individual droplets contribute to the accretion process. One approach has been to capture the moment of impact of a supercooled droplet onto a surface placed in an icing tunnel. However, this produces a large number of images that must be analysed manually. This paper describes the development of an automated analysis system, employing image processing techniques, that is capable of classifying the impact images without operator input. Using a carefully chosen feature vector and K-means clustering algorithm, the classification results from the automated system are comparable with that achieved using the manual approach.**

***Index Terms*—Aircraft Icing, Droplet Splash, Feature Extraction, Surface Classification**

I. Introduction

The topic of in-flight icing has been an important issue for many years. When aircraft fly through clouds or precipitation, icing will occur at temperatures below freezing. Given the importance of aviation flight safety, more research is required into in-flight icing. The two main fields being developed include large super-cooled water droplet impact for ice shapes prediction and understanding the ice accretion process for ice protection system. At Cranfield University, investigations are being carried out into the effects of super-cooled droplet impact splashes onto a simulated airfoil surface. The water droplets have similarity in size and speed in the ambient conditions relevant for super-cooled large droplet (SLD) icing. The term "SLD icing conditions" refers to the situation in which the cloud volume median diameter (VMD) is greater than 50μm and the water is cooled below zero Celsius degree but without freezing.[1]-[2], The material from which the airfoil surface is constructed plays an important role during ice formation process, as it may influence the extent to which water films build up. To monitor this process, image sequences are captured showing droplets impacting a test surface. In the past, images were manually classified, one by one, in accordance with droplet splash models to identify the surface conditions at the time of impact. However, due to the subjective nature and time consuming nature of manual classification, digital image processing techniques are being introduced to improve the image classification. In addition, image processing techniques allow a more objective classification of impact events. This paper describes the development and implementation of an automatic image classification scheme that allows sample surfaces to be categorized according to the presence of the water film. Specifically, attempts are made to differentiate between 'dry' and 'wet' surfaces.

This work was supported in part by the Cranfield Icing Research Center and the ADELINE project.

Xueqing Zhang , Applied Mathematics and Computing Group (AMAC), School of Engineering, Cranfield University, U.K. MK43 0AL (e-mail: selina.zxq@gmail.com).

Stuart Barnes (Corresponding author), AMAC, School of Engineering, Cranfield University, U.K MK43 0AL (Tel: +44 (0)1234 750111; e-mail: s.e.barnes.2002@cranfield.ac.uk).

David Hammond, School of Engineering, Cranfield University, UK. MK43 0AL (e-mail: d.w.hammond@cranfield.ac.uk)

II. Manual Image Classification of Droplet Splash

Before starting to implement specific image processing approaches, it is important to illustrate a few test cases as classification criteria for software validation. The images generated by experiment consisted of a side view of the target sample, which was inclined at an angle to the horizontal to encourage the liquid to run off. The droplet impacted the sample from above. An initial run of 200 training images were manually classified to validate the automated process. From this analysis, four classes were initially identified:

- Diffusion images – Dry surface
- Corona images – Wet surface
- Mixed events images –Ambiguous
- Useless images

However, there are a number of factors that make interpreting the images problematic. For example, the camera exposure, though constant (1ms), was not synchronized with individual impact events since exposure times were longer than the event duration. This means there is a chance that multiple droplets hit the target surface within the duration of the exposure, and in some cases, at the same location.

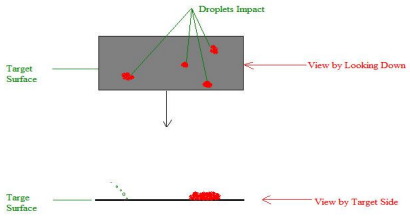

Figure 2.1 Multi-droplet impacts in different locations

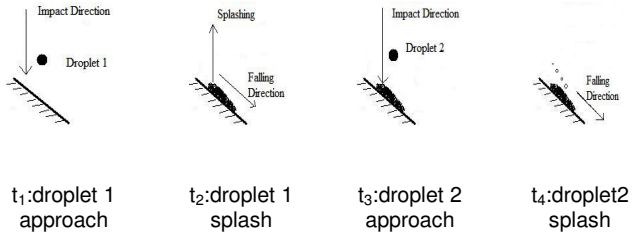

Figure 2.2 Multi-Droplets impact at different time

To illustrate typical scenarios we present some examples. Figure 2.1 represents four droplets which impact on a target surface at the same time, but at different locations. On the left hand side of target, we assume a water film has developed due to previous droplet impacts. The impact of another droplet onto the water film will result in a corona or the ejection of water droplets from the surface. On the right hand side, we assume that the interval since the last impact has been sufficient for any water film to have dissipated. Subsequently, when droplets strike this region we see a more diffuse behaviour. However, depending upon the surface conditions at the time of impact, it is possible that a mixture of these events may occur, making it difficult to correctly identify the sample from this information alone.

In Figure 2.2, the sequence of four images represents two droplets hitting a sloping target at different times at the same location. Initially, the sample surface is dry when droplet 1 impacts causing diffuse behaviour at time t_2. Droplet 2 impacts at the same location as droplet 1, but before the latter has had time to run off (t_3). The resulting splash image would then show wet behaviour for that surface.

Furthermore, we see samples that exhibit a limited buildup of surface water in the form of beads (figure 2.3a). In this scenario we can have a droplet impacting the beads, leading to what appears to be 'wet' surface behaviour (Figure 2.3b).

The mixed events category encompasses these scenarios, making it difficult to classify the images into 'wet' or 'dry' surfaces. In reality the material samples themselves could not so easily be classified into wet or dry, it being more likely that they would be characterized by a continuous value representing the likelihood of a film forming on their surface. However, for the purposes of identifying characteristics of the image, this classification is sufficient.

(a) droplet approach (b) droplet splash

Figure 2.3 Droplet Splash onto beading up surface

The remainder of this section will describe the four categories of impacting events, with an image used to illustrate each.

Diffusion Image

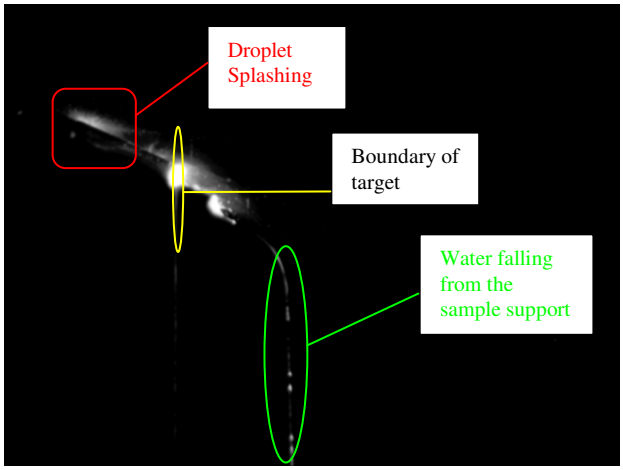

Figure 2.4 Diffuse mist due to dry surface

In Figure 2.4, ignoring anything to the right of the target boundary, we can focus on the droplet splashing region on the target surface. This form of this impact illustrates a droplet hitting a dry surface and producing a dense mist. This can be seen at the left-top corner of Figure 2.3. From this we classify a diffuse structure being related to a dry surface.

Corona Image

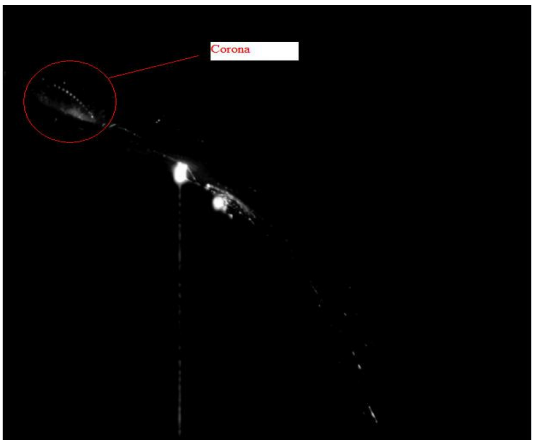

Figure 2.5 Corona structure indicating wet surface

Figure 2.5 shows a corona[3] structure which demonstrates how a larger droplet strikes a reasonably smooth water layer and produces a string of droplets pointing backwards out of the water layer. There may also be some diffuse aspect, but the coronal structure confirms this as a wet surface.

ISBN:978-988-98671-5-7

Mixed with diffusion and corona images

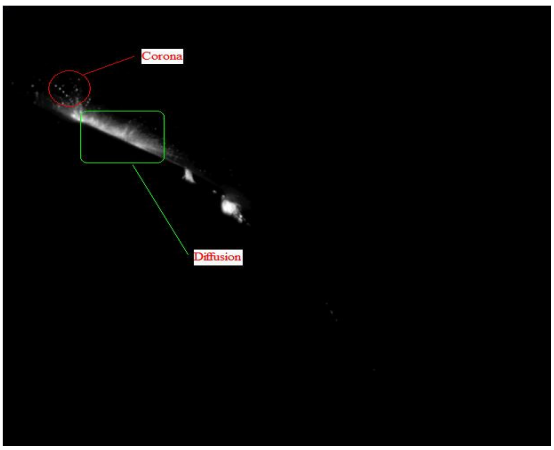

Figure 2.6 Mixed events

In Figure 2.6, it is a complicated impacting event. It has not only a diffusion section, but also a sequence of droplet points, namely the corona. How to characterize these mixed events' features becomes a big issue as part of this investigation. Image 309 shows that there is more than one droplet impacting onto the surface during the impacting period. In certain circumstances, it is possible that a little water remains on part of target, but the other region stays dry where no droplet hit. Therefore, when droplets impact onto different sections, the perspective in the 2D image displays a mixed event with both a diffusion area and the corona. In this case, it is rather difficult to distinguish whether the surface is wet or dry.

Useless images

Figure 2.7 Useless image 059

In Figure 2.7, the picture appears to have been captured at a point where no droplet has impacted the surface. There are no noticeable characteristics in the droplet splashing region. As a result, it is impossible to tell what, if anything, has occurred in this impact image.

In summary, when the images display a brighter diffusion region, it can be identified as dry surface. Meanwhile, the presence of backward corona is usually related to a wet surface. However, the corona sometimes has forward direction or the brightness is weak. The difficulty in detecting coronas rises in relation to the variable thickness of remaining water layer on the target surface [4] [5]. Mixed events are the most challenging classification among the four categories because of the complexity of distinguishing the wet or dry behaviour in the original image.

III. IMPLEMENTATION

The implementation was performed using the OpenCV image processing library and Microsoft Visual Studio with C++. Some additional steps, such as the classification stage, were performed using Matlab.

The processing chain for each image consisted of three steps: (i) pre-processing, (ii) feature extraction, (iii) classification. Pre-processing activities included masking off unnecessary parts of the image and applying Gaussian filtering to reduce artifacts from the image capture process. The important step of feature extraction allowed the identification and measurement of those aspects of each image that could be later used for classification. Finally, a K-means clustering method was used to determine which class the image fell into according to its feature vector. The K-means algorithm is one of the simplest unsupervised learning algorithms for solving clustering problems [7]. The choice of four classes used in the K-means was defined by the manual classification performed earlier.

There are a wide variety of techniques used for feature extraction. Statistical measurements are the fundamental approach taken here, which included average greyscale brightness, contrast, correlation, and entropy. From these, a feature vector was defined that also included Hough lines to add a structural aspect to the feature space.

Average Brightness

This operator can characterize the average of brightness within whole image. Equation 3.1 is described the operator to calculate average brightness.

$$f = \frac{\sum_{j=0}^{N_{height}} \sum_{i=0}^{N_{width}} p(i,j)}{N_{height} \times N_{width}} \qquad 3.1$$

where p(i, j) is the greyscale value of each pixel, N_{height} and N_{width} represent respectively value of height and width of source image.

Mean & Standard Deviation

The images are sub-divided into 25x25 windows, and the mean and standard deviation of each was calculated with following:

$$\overline{p} = \frac{\sum_{i=0}^{N} p(i)}{N_{height} * N_{width}} \qquad 3.2$$

$$\sigma_p = \sqrt{\frac{\sum_{i=0}^{N}(p(i)-\overline{p})^2}{N}} \qquad 3.3$$

where p(i) is the value of pixel, N_{height} and N_{width} are height and width of sub images, and N is the number of sub images.

Entropy

Here we use entropy to define the level of structure in each sub-window. It allows us to make a distinction between those areas of diffuseness and those in which a more definite structure exists. It is defined as:

$$\overline{E} = \frac{\sum_i \sum_j p(i,j)\log\{p(i,j)\}}{N} \qquad 3.4$$

with its associated standard deviation defined as:

$$\sigma_E = \sqrt{\frac{\sum_i (E(i)-\overline{E})^2}{N}} \qquad 3.5$$

where p(i, j) is the value of pixel of image, N is the number of sub images.

Ratio of Entropy

To further differentiate between wet and dry behaviour, a ratio was defined based on the entropy of each sub-window. We defined this ratio as follows:

$$ratio = \frac{n\_HEP}{n\_LEP} \qquad 3.6$$

where n_HEP is the number of sub-windows whose entropy is larger than 5000 per image, n_LEP is the number whose entropy is lower than 5000. The threshold was determined empirically, comparing the entropy between the sub-windows containing corona and diffusion features.

Hough Line

Although statistical metrics are useful, they do not identify specific structures within each sub-window. To provide extra structural information, we used the fact that the wall of the corona forms an angle with the surface of the target (Figure 3.1).

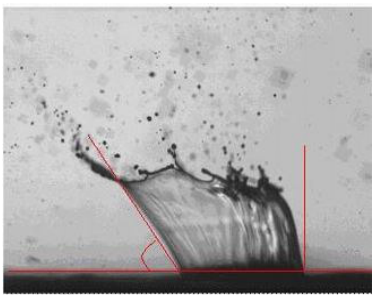

Figure 3.1 A typical corona shape

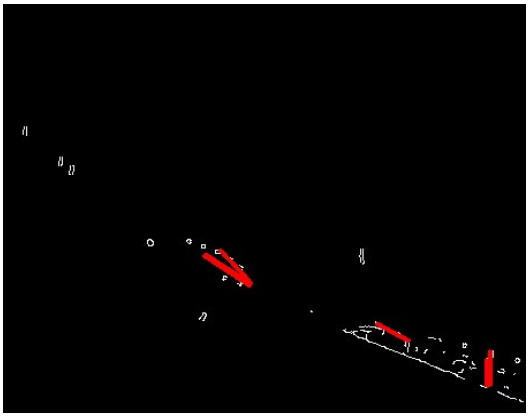

Figure 3.2 Probabilistic Hough Transform of Image 102

The Canny edge detection algorithm[6] was used to emphasize the edges of corona, and the Hough transform[6] was applied in order to detect the lines. The Hough routine returns a distance and an angle parameter which can be used to define another parameter set in the feature vector. Figure 3.2 shows an example of the Hough Transform detecting four lines which represent possible coronal structures.

Since we are not interested in any activity below the target surface, we can also mask out any Hough lines contained there by defining a threshold angle. The angle is dependent upon the experimental setup of the sample, and a typical set for 4 different samples is shown in Table 3.1 Thus, the detectable angle of any useful structure detected by the Hough routine should be in the approximate range $28° < \theta < 203°$, with any Hough lines outside of this range being discarded.

The corona is the key feature used to detect a wet surface. However, some ambiguous images appeared to show corona ejecta moving down the slope to the right with no left hand structure. To further improve the discrimination of wet images we targeted corona that displayed either both walls of the structure, or just the left-hand wall. Thus, we try to detect the 'backwards' corona with the angle between 28º and 90º, and calculate a ratio of the number of 'backward' lines compared with the total lines within the image. If the ratio is large, it indicates that the presence of a corona is more likely.

The full feature vector therefore includes the global image brightness, the sub-image brightness with its standard deviation, entropy of sub-image, standard deviation of entropy, ratio of entropy, and Hough lines with the ratio of backward lines compared with total Hough lines.

Group	Hough Angle
A: Image 1- 78	22.5º
B: Image 79-84	22.3º
C: Image 85-95	24.17º
D:Image 96-662	24.19º

Table 3.1 Target surface Hough angle

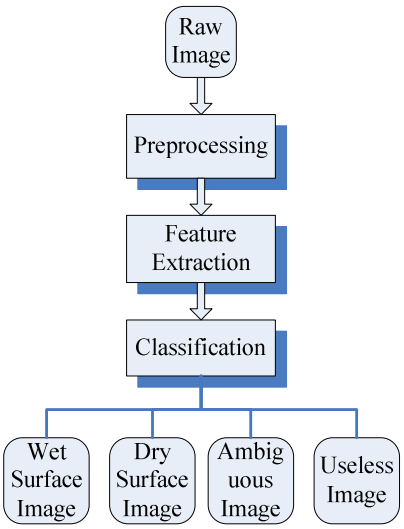

Figure 3.3 Processing algorithm

IV. RESULTS AND DISCUSSION

The 200 manually validated images were processed using the automated algorithm (Figure 3.3). The metrics defined in the previous section were calculated for each image, and the resulting feature vector then used to categorize the image into one of the four classes using the K-means clustering method.

The initial feature vector used to classify the images contained a total of eight metrics. However, analysis of the results showed that there was insufficient detail in each image to distinguish between the values of the global greyscale mean and the individual sub-window means. Furthermore, the standard deviation of the sub-window greyscale values also showed insufficient discrimination of the results to justify its inclusion in the feature vector. As a result, both of these sub-window metrics were dropped from the final feature vector. The final form of the feature vector comprised of:

- Global average greyscale brightness
- Average sub-window entropy
- Standard deviation of sub-window entropy
- Ratio of entropy
- Hough line angle
- Ratio of Hough lines

After the normalization of feature space values, the output of the classification stage categorized the images into the four groups: dry surface, wet surface, ambiguous images and useless images. Figure 4.1 shows how the images are sorted into the four groups, using only two of the feature metrics: average brightness and ratio of Hough Lines. We can see that the images fall into the four categories with relatively little overlap. Using additional parameters of the feature vector increased the discrimination between groups still further.

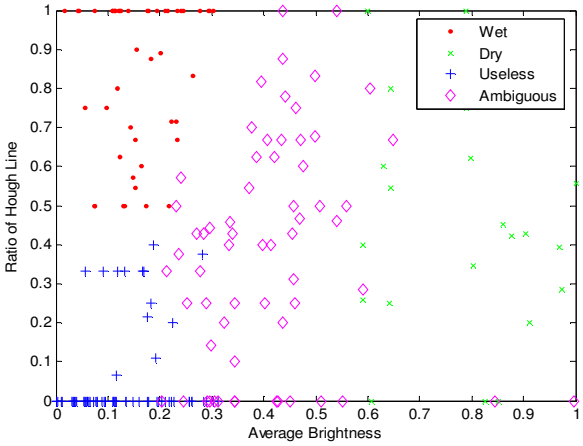

Figure 4.1 Classification of 200 Images in 2D space

The ratio here shows the number of Hough lines with the angle between 28º and 90º, compared to the total Hough lines. The "+" group represents the useless images as they all have lower brightness and no Hough lines. Besides, the "." group has a greater ratio of Hough Lines with lower brightness, which can be interpreted as wet surface category. The "x" and "◊"group has a greater brightness which illustrates the diffusion in the images. The "◊" group shows that the images also detected Hough lines, so that we can define these as ambiguous images, with the remaining group being the dry surface category.

When we define the structure of feature space as entropy, ratio of entropy and ratio of Hough Lines, we can see the images still separate into four categories (Figure 4.2). The ratio of entropy represents the comparison between dry surface and wet surface in the 25x25 sub-images. The green group represents the dry surface as its entropy and the ratio is greater, which means those images have a large area of diffusion part. The other groups have similar characteristics as with Figure 4.1.

Table 4.1 shows the comparison of the automatic classification and the manual classification. Roman numerals are used to represent the four cluster categories in the automatic analysis. In the manual analysis, 'D' stands for dry surface, 'W' stands for wet surface, 'A' stands for ambiguous group, and 'U' for unusual images.

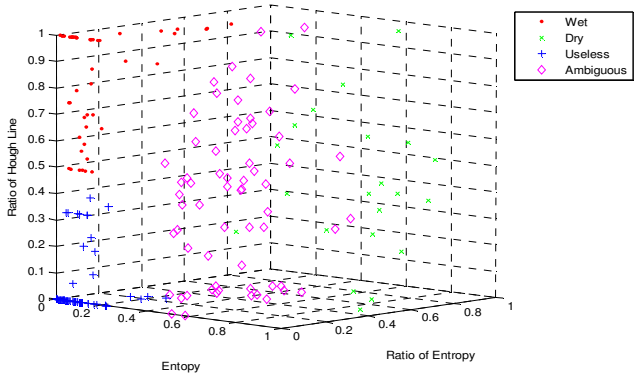

Figure 4.2 Classification of 200 images in 3D space

Automatic Category	Manual Category
I	32 'W', 5 'U', 9 'A'
II	14 'D', 8 'A'
III	8 'W',1 'D', 43'U', 13'A'
IV	3 'W',24'D', 1'U', 36 'A',

Table 4.1 Formation of 200 images classification

Each of the images assigned to an automatic group has its corresponding manual classification added to the second column of Table 4.1. For example, of the images assigned to group I, the manual classification showed that 32 of these were assigned as 'wet'. Hence, from the table, group I and II seem to be related to wet surface and dry surface images respectively. Although it is difficult to clarify category III and IV, we can assume that group III represents the useless category and IV is related to ambiguous images. Finally, comparing the number of each cluster with total training test images, the classification results are shown in Table 4.2.

We can see that the automatic classification is comparable to the manual results, with a few discrepancies, the most notable being that of the 'dry' classification. Examining the corresponding images shows that many images that should have been categorized as 'dry' were designated as 'ambiguous' by the automated system. This is due to the low brightness values in the diffuse areas, as is demonstrated in Figure 4.1. Further optimization of the feature vector should improve these results and this remains an area for future work.

V. CONCLUSION

A methodology has been developed that automatically classifies images previously captured during a super cooled large droplet splash experiment. This reduces the necessity for manual analysis, which can be both time consuming and prone to subjective interpretation.

The set of feature metrics used as part of the image processing included greylevel brightness, sub-window entropy and identification of structures using the Hough transform.

Category		Ratio(member / total image)	
		Automatic Classification	Manual Classification
I	Wet surface image	23.3%	21.8%
II	Dry surface image	11.2%	19.8%
III	Useless image	33.0%	24.9%
IV	Ambiguous image	32.5%	33.5%

Table 4.2 Classification of automatic and manual systems

Using a manually validated test set of images, the automated method has been successful in correctly classifying them into wet, dry, ambiguous or useless groups. Results have shown that the outcomes from the automated and manual classifications are broadly comparable, although further optimization of the feature vector could improve the results still further.

REFERENCES

[1] "Aircraft Icing handbook" Civil Aviation Authority 2000, p. 1-20.
[2] Gent, R.W., Dart, N.P. and Cansdale, J.T. "Aircraft Icing". *Phil. Trans. R. Soc. Lond*. 2000, 358, 2873-2911
[3] Hammond, D.W. "Investigation into Super cooled Large Droplet Splashing". Commissioned by the CAA (contract 623), March, 2005. (to be published)
[4] Luxford G, Hammond D, & Ivey P, "Modelling, Imaging and Measurement of Distortion, drag and Break-up of Aircraft-icing Droplets", *presented at the AIAA 43rd Aerospace Sciences Meeting and Exhibition, Jan 2005, Reno, AIAA Paper 2005-0071*
[5] Hammond D W, Quero M, Ivey P, Miller D, Purvis R , McGregor, O & Tan J, "Analysis and Experimental Aspects of the Impact of Supercooled Water Drops into Thin Water Films", *presented at the AIAA 43rd Aerospace Sciences Meeting and Exhibition, Jan 2005, Reno, AIAA Paper 2005-0077*
[6] Mark S. Nixon,Alberto S. Aguado. "Feature Extraction and Image Processing" Newnes, (First Edition) 2002.
[7] Andrew Webb. "Statistical Pattern Recognition" Butterworth Heinemann, Second Edition 2002.